COMPUTER VISION BASED SURVEILLANCE CONCEPT FOR AIRPORT RAMP OPERATIONS

Sai Vaddi & Hui-Ling Lu, Optimal Synthesis Inc., Los Altos, CA
Miwa Hayashi, NASA Ames Research Center, Moffett Field, CA

Abstract

Current research develops a vision-based surveillance system concept suitable for airport ramp area operations. The surveillance approach consists of computer vision algorithms operating on video streams from surveillance cameras for detecting aircraft in images and localizing them. Rough order of magnitude estimates of the number of cameras required to cover the ramp area at a sample airport (Dallas/Fort Worth International Airport) were obtained. Two sets of algorithms with complimentary features were developed to detect an aircraft in a given image. The first set of algorithms was based on background subtraction, a popular computer-vision approach, for change detection in video streams. The second set was a supervised-learning approach based on a model learned from a database of images. The Histogram of Oriented Gradient (HOG) feature was used for classification with Support Vector Machines (SVMs). Then, an algorithm for matching aircraft in two different images was developed based on an approximate aircraft localization algorithm. Finally, stereo-vision algorithms were used for 3D-localization of the aircraft. A 1:400 scale model of a realistic airport consisting of a terminal building, jet bridges, ground marking, aircraft, and ground vehicles was used for testing the various algorithms. Aircraft detection was demonstrated using static and moving aircraft images, single and multiple aircraft images, and occluded aircraft images. Preliminary testing using the in-house setup demonstrated 3D localization accuracy of up to 30 ft.

Introduction

Ramp areas in airports are densely occupied by aircraft, ground vehicles, and ground crew. At most airports ramp areas are not covered by surveillance systems such as RADAR and Airport Surface Detection Equipment - Model X (ASDE-X). Even when surveillance systems such as Automatic Dependent Surveillance -Broadcast (ADS-B) are available they require the aircraft avionics to be powered *on*, whereas some aircraft in the ramp area may have the avionics system turned *off*. Another drawback of surveillance technologies in ramp area is that technologies, such as RADAR and Global Positioning System (GPS) based ADS-B, suffer from multi-path errors in the ramp area thus compromising the accuracy [1].

The proposed vision-based surveillance system overcomes the above obstacles as it does not require any aircraft equipage and participation. It is a ground-based passive surveillance system. Therefore, it does not suffer from multi-path errors.

Vision-based surveillance systems have found significant applications in monitoring the security of public places as well as private businesses. However, in these applications they typically aid the humans by combining the feeds from multiple cameras into a single view for the monitoring personnel. In other applications, vision based approaches have been used for road surveillance [2]. Refs. [3] and [4] specifically deal with vision-based surveillance approaches for airport surface traffic. However, the functional, algorithmic, and performance details of these concepts specifically applied to the densely populated ramp area, are not available at the moment for comparison.

Surveillance in ramp area has multiple benefits:

- Surveillance information can enable safety monitoring systems (such as Refs. [5], [6]) for ramp area operations. The Flight Safety

Foundation estimates that 27,000 accidents occur on airport ramps worldwide each year, and 243,000 people are injured, or roughly one injury for every 111 departures [7]. Industry experts put the airlines' cost due to ramp area accidents at $4 billion to $5 billion internationally each year [8].

- Real-time surveillance updates could aid in better planning gate release and ramp spot release/sequence operations by planners such as the Spot and Runway Departure Advisor (SARDA) [9] by providing real-time updates on the pushback and taxi status of the aircraft. SARDA was developed by the Safe and Efficient Surface Operations (SESO) group at NASA Ames Research Center.

Figure 1 shows the functional architecture of the proposed concept. The primary inputs come in the form of video streams from surveillance cameras. Auxiliary inputs are the schedule data, and other surveillance information, if any. The first set of algorithmic modules processing the video data consists of the 'Aircraft and Ground Vehicle Detection' modules (purple colored blocks in Figure 1). The purpose of these modules is to detect the presence of aircraft or ground-vehicles in a given image frame. The second module is the aircraft localization module whose task is to estimate the 3D location of the aircraft in an inertial frame of reference. This is done in two sub-modules: (i) Aircraft Matching, and (ii) 3D-Localization (orange colored blocks in Figure 1). The Aircraft Matching module matches the aircraft identified in image frames obtained from different cameras. The 3D-Localization module uses stereo-vision algorithms to estimate the 3D location using two images of the same aircraft obtained from two different cameras.

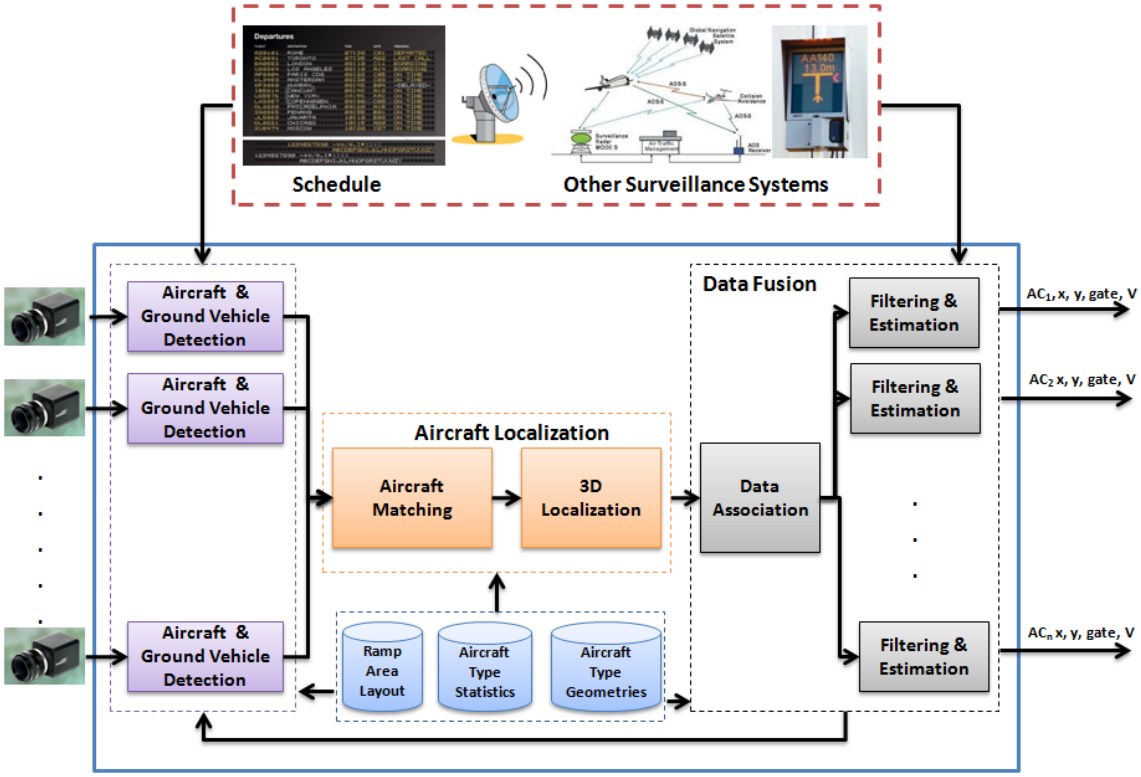

Figure 1. Functional Architecture of the Proposed Concept

The last module is the Data Fusion Module (gray colored blocks in Figure 1) which deals with tracking aircraft over multiple cameras. This involves data-association and state estimation algorithms. The blue colored blocks indicate data sources that could aid the overall system. The overall output from the

surveillance system consists of aircraft ID; position coordinates of the aircraft x, y; gate where the aircraft is parked; speed V and heading χ if the aircraft is moving. Advanced vision-based algorithms are also capable of generating aircraft orientation information.

Apart from the surveillance mode, the proposed system can be used in a post-processing mode to conduct surveillance video data analysis. In this mode the proposed system can identify the paths taken by aircraft in the ramp area; model the statistics of time taken by aircraft to move from gate to ramp spot; identify special events of interest such as simultaneous push back from adjacent gates.

Camera Requirements

The following are design parameters of a camera-based surveillance system:

- Wave length of operation (e.g., Visible, Infrared, which is suitable for night-time and low-visibility operations)
- Number of cameras
- Location & orientation of cameras
- Focal length (f) of the cameras
- Imaging sensor size (s) of the cameras
- Resolution of the imaging sensor
- Type of lens (e.g., Wide Angle, Fish eye, Panoramic)
- Degrees of freedom (i.e., Pan, Tilt, and/or Zoom).

A pin-hole camera model (Figure 2) is used to compute the approximate number of cameras required to provide complete coverage for a sample airport, Dallas/Ft. Worth International Airport (DFW).

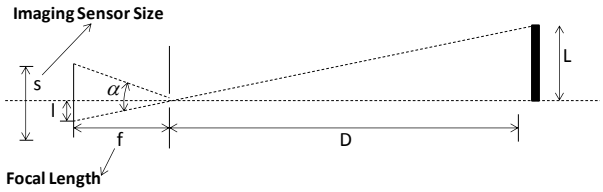

Figure 2. Pinhole Camera Model

The following is the basic equation that describes the perspective transformation resulting from a camera. An object of length, L, at a distance, D, from the camera is shrunk to a length, l, which is dependent on the focal length of the camera, f.

$$l = \frac{fL}{D} \tag{1}$$

The field-of-view of a camera is an important parameter that determines the geographical area captured by the camera. It depends on the focal length, f, and the size of the imaging sensor, s, and is typically characterized by the angle, α.

The total number of cameras required to cover the complete ramp area depends on the area of the ramp represented by $Area_{ramp}$, and the maximum area captured by a single camera $Area_{max}$. It can be approximated by the following equations:

$$n_{cameras} \approx \frac{Area_{ramp}}{Area_{max}} \tag{2}$$

$$Area_{max} = 4kL_{max}^2 \tag{3}$$

where k is the length to width ratio of the imaging sensor; and L_{max} is the maximum object length that could be captured by a camera at a distance D.

$$L_{max} = D \tan \alpha \tag{4}$$

It should be noted that the above equation is an approximation. It assumes no occlusions and assumes the feasibility of placing the cameras at specified distance, D. The actual number of cameras could be higher. However, the above equation provides valuable insight into the camera requirements as explained by the following relations:

$$n_{cameras} \propto \frac{1}{D^2} \tag{5}$$

$$n_{cameras} \propto \frac{1}{\tan^2(\alpha)} \tag{6}$$

Typical sensor sizes could range from a minimum of 4mm in width to a maximum of up to 36mm. The focal length of cameras can vary from as low as 2.5mm to as high as 1m. Corresponding fields of view could vary between 50 degrees to 150 degrees. Figure 3-Figure 4 illustrate the number of camera requirements for cameras with different FOVs.

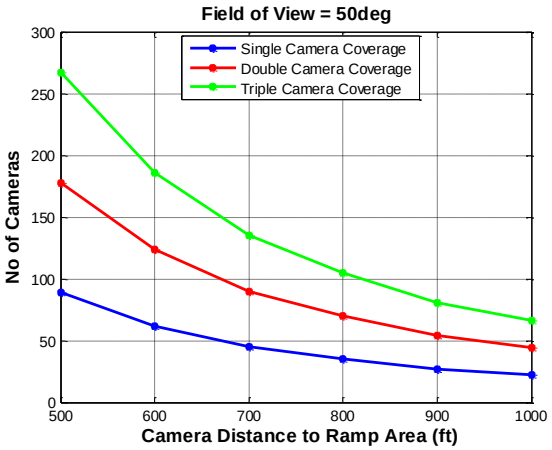

Figure 3. Required Numbers of Cameras with 50deg FOV Cameras

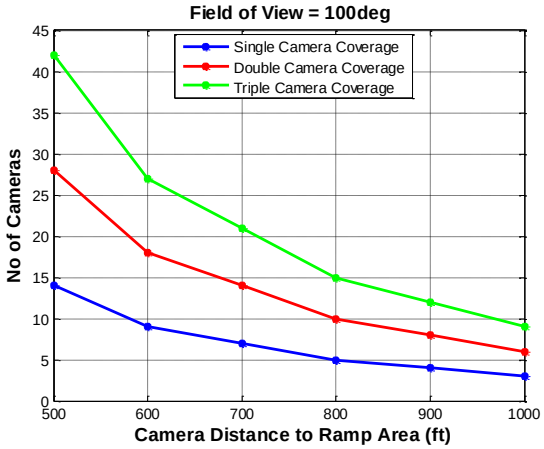

Figure 4. Required Numbers of Cameras with 100deg FOV Cameras

The three plots within each figure indicate the number of cameras required for single-camera coverage, double-camera coverage, and triple-camera coverage. Single-camera coverage refers to a scenario where each point is only viewed by a single camera. For purposes such as 3D-localization it is desired that the same aircraft be imaged by at least two cameras (double-camera coverage). Multiple cameras looking at the same aircraft from different angles also increases the robustness of aircraft detection.

The hyperbolic nature of the plots indicates the inverse proportionality with the square of the distance D^2 from the camera. It can also been seen by comparing Figure 3 and Figure 4 that doubling the FOV more than halves the number of cameras.

From these figures it can be concluded that for a 50 degree field-of-view camera placed 1000 ft from the area of interest could require as many as 50 cameras for double-camera coverage for a ramp area whose size is same as that of the DFW ramp area. It should be noted that DFW has relatively large ramp areas. Smaller airports could require less than half this number. It should also be noted that the above analysis does not take into account camera placement restrictions and occlusions. It is intended to be an approximate analysis to get a rough order of magnitude estimate of the number of cameras required for the proposed surveillance system.

Aircraft Detection Module

The role of this module is to sample each video frame and evaluate if an aircraft is present in the frame. Two different algorithms (i) Background-Subtraction Algorithm and (ii) Supervised-Learning Algorithm were developed for this purpose. The following sub-sections present the approach and the results obtained using the two algorithmic approaches.

Background-Subtraction Algorithm

The Background-Subtraction approach relies on the following premises: (i) The camera view is fixed. (ii) The scope of view consists of two components: (a) static terminal component, and (b) dynamic moving components. (iii) The dynamic moving components consist of aircraft, ground vehicles, and ground crew. (iv) Approximate sizes of the aircraft, ground vehicles, and ground crew are known.

Figure 5 shows a block diagram of this algorithmic approach. The inputs to this algorithm are an image of the background, and a sample image that may or may not contain an aircraft. The first step involves differencing and thresholding the difference to identify pixels whose values deviate from the background (see Figure 6). The second step involves clustering these pixels using K-Means algorithm (see Figure 7). The third step involves identifying the 3sigma ellipsoids associated with each cluster (see

Figure 8). The last step involves discarding small and low-density clusters, as well as combing nearby clusters (see Figure 9).

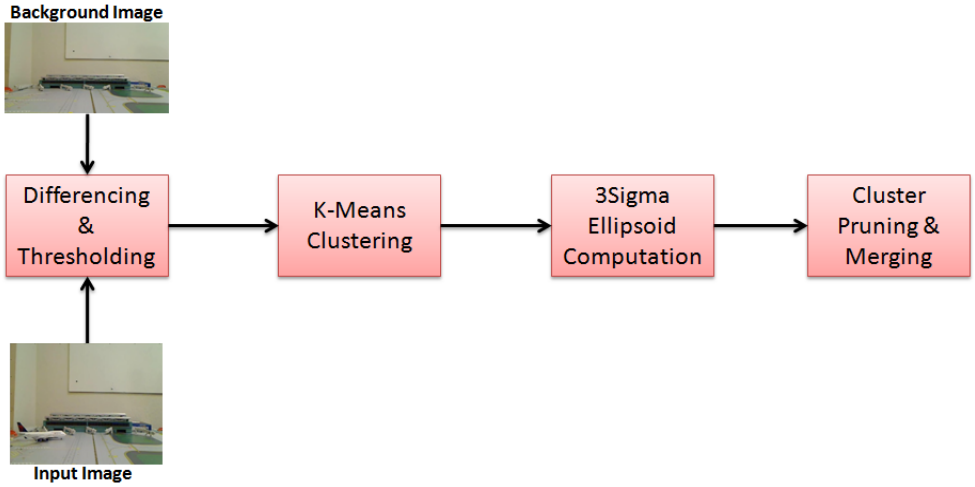

Figure 5. Functional Flow Diagram of the Background-Subtraction-Based Approach

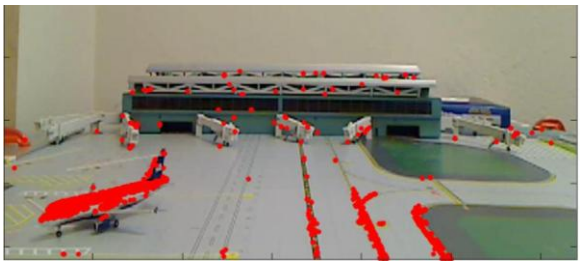

Figure 6. Difference Image

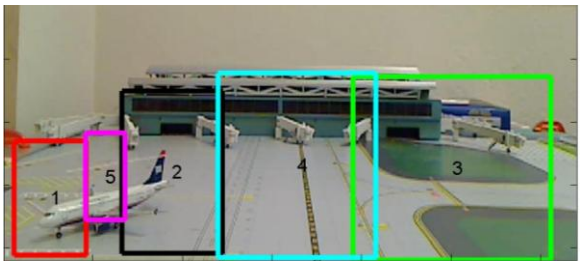

Figure 7. K-Means Clustered Image

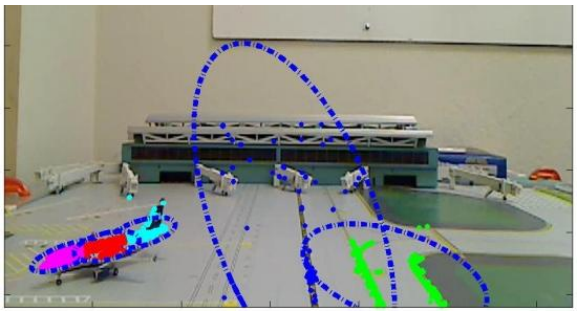

Figure 8. Image with Cluster 3Sigma Ellipsoids

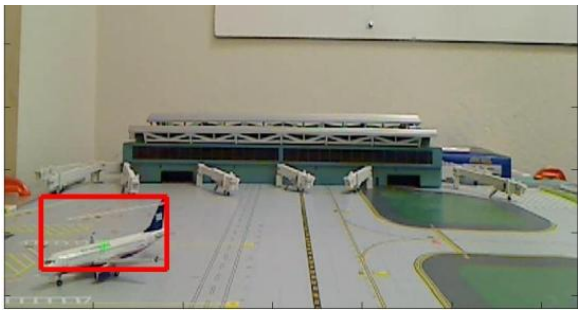

Figure 9. Final Image with Bounding Box

Results obtained applying the Background-Subtraction approach to pictures of a 1:400 scale model of an airport are shown in Figure 10-Figure 19. The results include different aircraft types, different orientations, and different locations. Figure 14-Figure 17 show multiple aircraft detection as well. Figure 17 and Figure 18 demonstrate detection amidst ground vehicles. It should be noted that the ground vehicles were not part of the background.

One of the challenges of the Background Subtraction approach is the ability to deal with changing lighting conditions of the background. Another challenge emanates from the fact that it may not be possible to get a background image without any aircraft or ground vehicles in the image. Results

presented here are based on a rudimentary background subtraction algorithm. Several advanced versions [10], [11] of Background Subtraction algorithms are available in literature that address both the above mentioned issues. Background is constantly updated in these approaches to accommodate the changing lighting conditions as well as moving aircraft. These algorithmic features will be evaluated in future research with actual surveillance video streams.

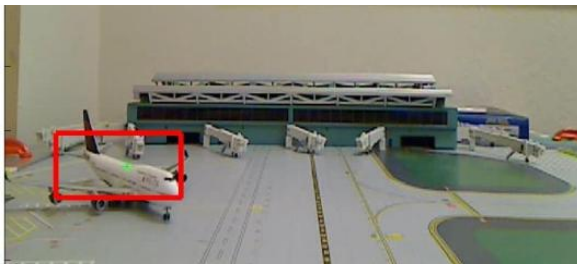

Figure 10. B747 Front View

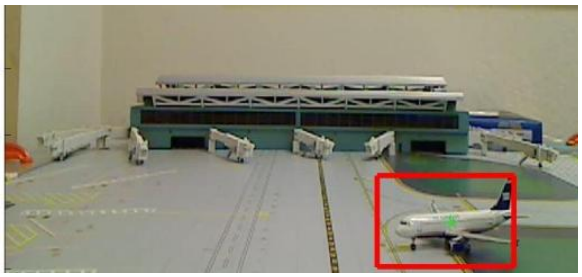

Figure 11. A320 Side View

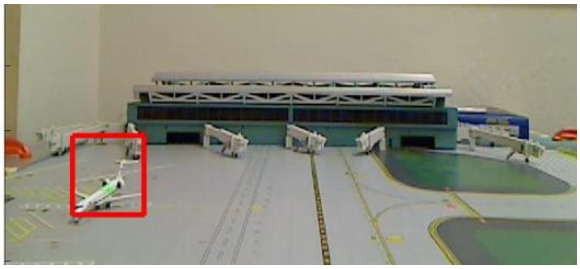

Figure 12. CRJ7 Front View

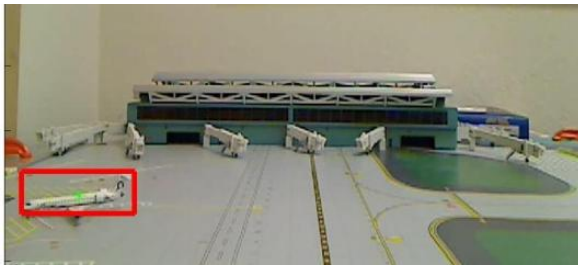

Figure 13. CRJ7 Side View

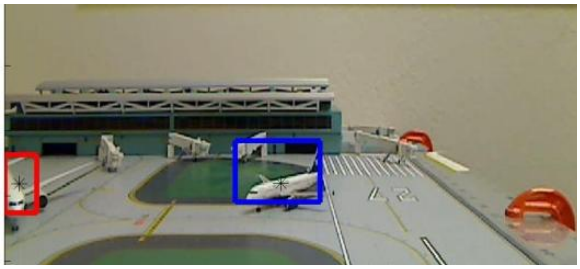

Figure 14. Detection of 2 Aircraft (B777 and A320)

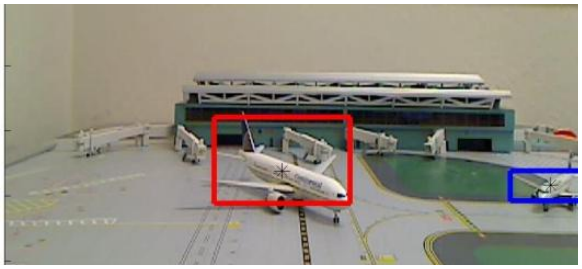

Figure 15. Detection of 2 Aircraft (B777 and A320)

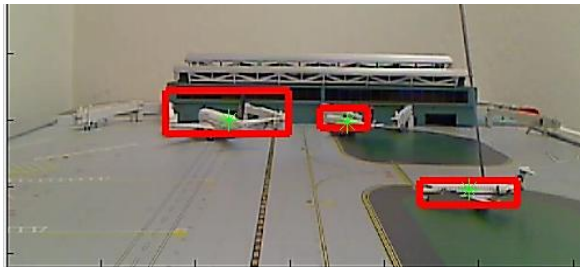

Figure 16. Detection of 3 Aircraft (B777, A320, CRJ7)

Figure 17. Two Aircraft (B777 and A320) and Ground Vehicles

Figure 18. B777 Pushback with Ground Vehicles

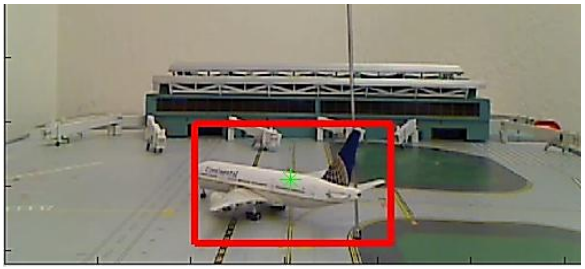

Figure 19. B777 Arrival at Gate

Supervised-Learning Algorithm

Another set of aircraft detection algorithms was built based on Discriminatively Trained Deformable Part Models (Refs. [12], [13]). This aircraft detection system does not require any prior assumption regarding the aircraft to be detected. Instead, it relies on pre-learnt aircraft models to infer the existence of the aircraft in the input image. The output is a binary variable indicating the presence of an aircraft; a bounding box representing the image plane location of the aircraft; and a coarse orientation angle.

During the learning stage, we construct the aircraft models from a database which contains aircraft of different types taken at various view-points. The Histogram-of-Orientation-Gradient (HOG) [14] feature is used for training purposes. The HOG feature is robust to scale and illumination variations. Figure 20 illustrates the calculation of the HOG feature for a single cell with the dimension of 8 by 8. HOG, as the name suggests, deals with a histogram of gradients. The gradients can be computed along the x axis, y axis or other directions as well. Once the gradients are computed over several pixels the information is encapsulated into a histogram representation. The histogram representation obviates the necessity to exactly compute the edges. It instead relies on the overall distribution of edge or gradient orientations at pixel level. The overall distribution (or histogram) tends be more robust to scale and illumination variations.

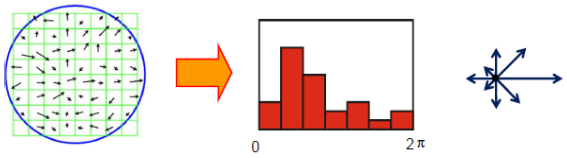

Figure 20. Computation of the HOG Feature

During the detection stage, the aircraft detection system scans through the image and queries the existence of the aircraft via the pre-built classifier which utilizes the aircraft model information. Support Vector Machine (SVM) framework is used for inference in Refs. [12], [13].

A few snapshots of the results obtained from the supervised-learning algorithm are shown in Figure 21-Figure 24. These results are for four different aircraft types in different views.

The success of learning-based approaches is dependent on the quality and quantity of the training data used. However, SVM aided learning approaches remain one of the most successful computer-vision approach for object detection. Whereas, the generic computer-vision problem seeks to identify a wide-variety of objects from a wide-variety of backgrounds the current problem is more focused. In that, it is based on a fixed camera location; restricted to detection of aircraft; and can also be adapted to individual ramp area for improved detection efficiency. These issues will be addressed in future research.

Figure 21. B747 Front View

Figure 22. B747 Side View

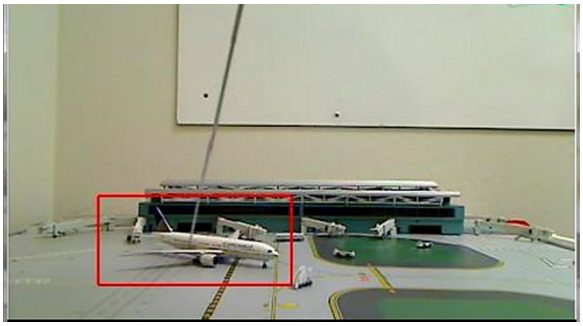

Figure 23. B777 Side View

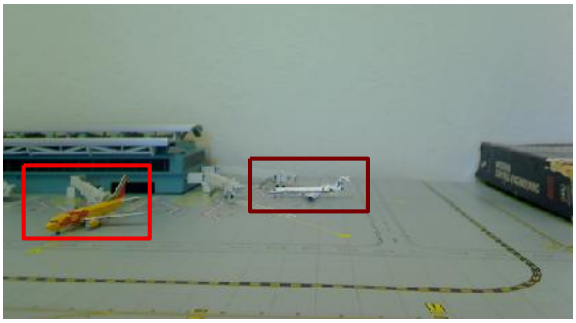

Figure 24. B737 AND CRJ700

Aircraft Detection Algorithm Comparison

The previous two sub-sections described two different algorithms for aircraft detection. The success of proposed vision-based surveillance system is crucially dependent on the success of the aircraft detection module. It should be noted that these two algorithms have different strengths and weaknesses. The background-subtraction approach is simple and takes advantage of the continuous video information but requires the accurate maintenance of background information. The supervised-learning approach benefits from the large number of trained aircraft examples. Specifically, the HOG feature is robust to scale and illumination variations. However, it requires a large amount of training data to generate accurate results.

Aircraft Matching Module

The first step in 3D-localization using stereo-vision is to match aircraft obtained from different cameras. This problem is referred to as '*Image Correspondence*' in computer vision parlance. In the context of the current research the problem is defined as follows: "Given two images, each containing an aircraft bounding box, are these two aircraft the same?".

An algorithm that is based on approximate aircraft localization is used in this research for matching aircraft in two different images. An approximate location of the aircraft is computed based on a single aircraft image. Figure 25 shows the Cartesian coordinate system used in this research. It should be noted that the Z axis matches the optical axis of the camera and captures the depth coordinate of the aircraft from the camera; the $X-Y$ plane matches the image plane; and the Y coordinate represents the height coordinates of the aircraft with respect to the ground.

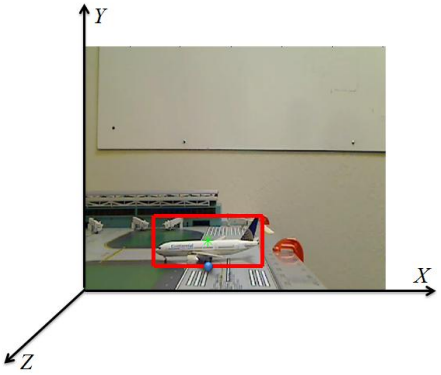

Figure 25. Cartesian Coordinate System Used for Aircraft Localization

The approach is based on the following premises: (i) All aircraft in the ramp area are on the ground, (ii) The lower horizontal edge of the bounding box represents points that correspond to the lower most parts of the aircraft, i.e., wheels, whose inertial frame Y-coordinates are zero ($Y_{LM1}, Y_{LM2} = 0$), where the subscript LM refers to lower mid-point (shown as blue dot in Figure 25), the subscripts 1 and 2 refer to cameras 1 and 2 respectively.

The premise (ii) is approximate because the bounding box in certain views cannot capture the bottom most portion of the aircraft. However, this approximation is not severe because the vertical (height) dimensions of the aircraft are much smaller (< 100 ft, which makes the error much smaller than 100 ft) compared to the X and Z dimensions which could be on the order of 1000 ft.

Using the above two premises the following equation was used to solve for the Z coordinate of the lower horizontal edge of the aircraft bounding box.

$$Z_{LM} = Z_c + \left(\frac{y - o_y}{f_y Y_c}\right) \tag{7}$$

$$X_{LM} = X_c - \frac{(x - o_x)(Z_{LM} - Z_c)}{f_x} \tag{8}$$

where the symbols X, Y, Z with subscript LM refer to the coordinates corresponding to the lower mid-point of the bounding box, x, y pixel coordinates of LM point; symbols X, Y, Z with subscript c refer to the coordinates of the location of the camera, o_x , o_y are the coordinates of the image-plane centers, f_x, f_y refer to focal length per unit pixel width along x and y image planes axes,

$$f_x = \frac{f}{s_x} \quad f_y = \frac{f}{s_y} \tag{9}$$

where s_x and s_y are the imaging sensor pixel dimensions.

The following logic is used to determine if the aircraft identified in two different images obtained from two different cameras are the same:

(i) Compute X_{LM1}, X_{LM2} and Z_{LM1}, Z_{LM2} for both the bounding boxes

(ii) Compute the distance d between the two lower mid-points as follows:

$$d = \sqrt{(X_{LM1} - X_{LM2})^2 + (Z_{LM1} - Z_{LM2})^2} \tag{10}$$

(iii) Use the following logic to determine if the aircraft are the same or different: If d is less than a pre-defined threshold the two aircraft are considered the same, else, different.

Figure 26-Figure 35 demonstrate the results obtained by applying the above described aircraft matching logic. The two columns of figures represent images taken using two cameras located at different positions. The left column indicates the picture taken using the left camera and the right column represents the picture taken with the right camera. It can be seen from the bounding boxes that the aircraft are detected in all the images. Moreover, the aircraft matching logic successfully identified the matching aircraft pairs and rejected the mismatched ones.

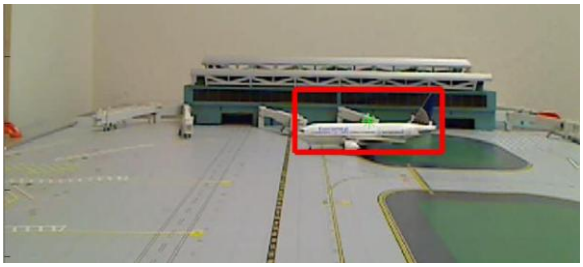

Figure 26. Left Camera Image

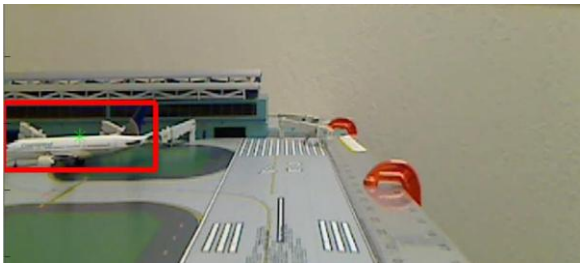

Figure 27. Matched Right Camera Image

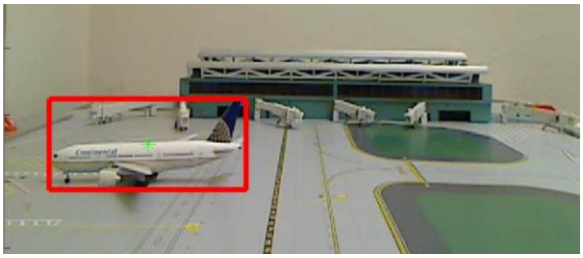

Figure 28. Left Camera Image

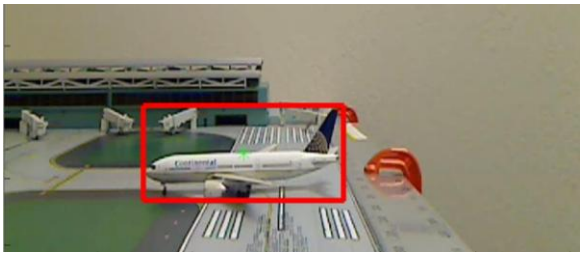

Figure 29. Unmatched Right Camera Image

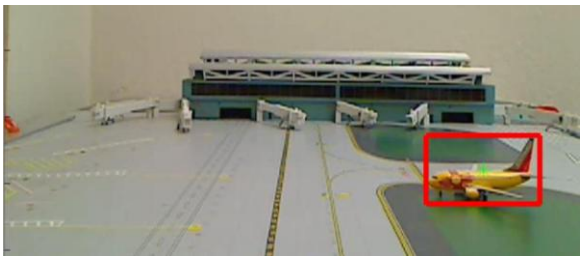

Figure 30. Left Camera Image

Figure 31. Unmatched Right Camera Image

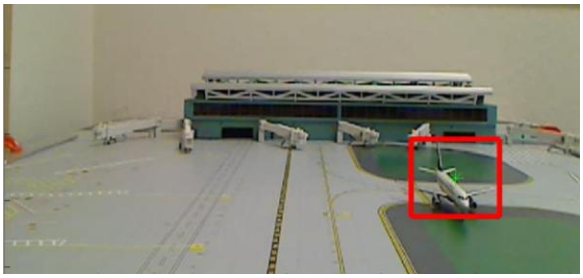

Figure 32. Left Camera Image

Figure 33. Matched Right Camera Image

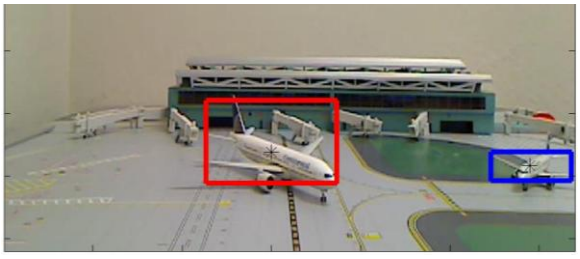

Figure 34. Left Camera Image

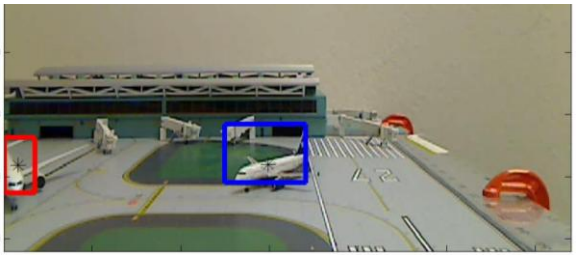

Figure 35. Matched Right Camera Image

Aircraft Localization Module

The objective of this module is to compute the 3D position coordinates (X, Y, Z) corresponding to the centroid of an aircraft in an inertial reference frame.

Inputs are:

- The pixel coordinates (x_1, y_1) and (x_2, y_2) of the centroids of two matched aircraft obtained from two different cameras. The centroids of the bounding boxes are treated as the centroids of the aircraft.
- The locations of the two cameras are (X_{c1}, Y_{c1}, Z_{c1}) and (X_{c2}, Y_{c2}, Z_{c2}).
- The intrinsic parameters of the cameras $(o_{x1}, f_{x1}, o_{y1}, f_{y1})$ and $(o_{x2}, f_{x2}, o_{y2}, f_{y2})$.

Outputs are 3D position coordinates (X, Y, Z) of the aircraft centroid.

The following equations are valid for the projection of a point (X, Y, Z) on to the image planes. The subscripts 1 and 2 refer to Camera 1 and Camera 2 respectively.

$$x_1 = o_{x1} - f_{x1}\left(\frac{X - X_{c1}}{Z - Z_{c1}}\right) \tag{11}$$

$$y_1 = o_{y1} - f_{y1}\left(\frac{Y - Y_{c1}}{Z - Z_{c1}}\right) \tag{12}$$

$$x_2 = o_{x2} - f_{x2}\left(\frac{X - X_{c2}}{Z - Z_{c2}}\right) \tag{13}$$

$$y_2 = o_{y2} - f_{y2}\left(\frac{Y - Y_{c2}}{Z - Z_{c2}}\right) \tag{14}$$

The above equations can be rearranged into the following matrix form:

$$\begin{bmatrix} f_{x1} & 0 & (x_1 - o_{x1}) \\ f_{x2} & 0 & (x_2 - o_{x2}) \\ 0 & f_{y1} & (y_1 - o_{y1}) \\ 0 & f_{y2} & (y_2 - o_{y2}) \end{bmatrix} \begin{bmatrix} X \\ Y \\ Z \end{bmatrix} = \begin{bmatrix} f_{x1}X_{c1} + Z_{c1}(x_1 - o_{x1}) \\ f_{x2}X_{c2} + Z_{c2}(x_2 - o_{x2}) \\ f_{y1}Y_{c1} + Z_{c1}(y_1 - o_{y1}) \\ f_{y2}Y_{c2} + Z_{c2}(y_2 - o_{y2}) \end{bmatrix} \tag{15}$$

Given the intrinsic parameters and locations of the cameras, and pixel coordinates of the same point in both the images, it is possible to solve the above system of linear equations for the 3D location of the point (X, Y, Z). A single camera only results in two equations (say equations 11 & 12, or 13 & 14) in three unknowns X, Y, and Z. Therefore, a unique solution cannot be obtained. Having multiple cameras creates more constraints (or equations) on the three unknowns X, Y, and Z resulting in a more accurate solution.

Figure 36, Figure 37, and Figure 38 show the aircraft localization accuracy along the X, Y, and Z axes respectively. The 3D-position localization accuracy is shown in Figure 39. These errors are obtained from 16 different aircraft localization tests. The x-axis refers to the test number. The errors shown here are scaled up 400 times to map the results of 1/400 scale model into a real-world setting. It should be noted that the maximum errors in these figures are less than 30 ft, which is small compared to the size of the ramp area and the size of the aircraft. The errors in these figures are computed as Actual Values - Estimated Values. The biases in the figures reflect in part the inability to measure the Actual Position of the aircraft in the camera coordinate system. This is in turn due to the fact that the origin of the coordinate system which is attached to the imaging sensor could only be approximately located in the cameras used under the current research. The biases however can be estimated and rejected through a calibration process.

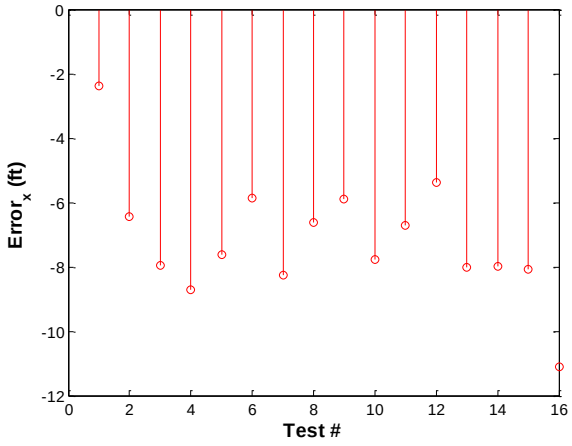

Figure 36. Localization Accuracy along X-Axis

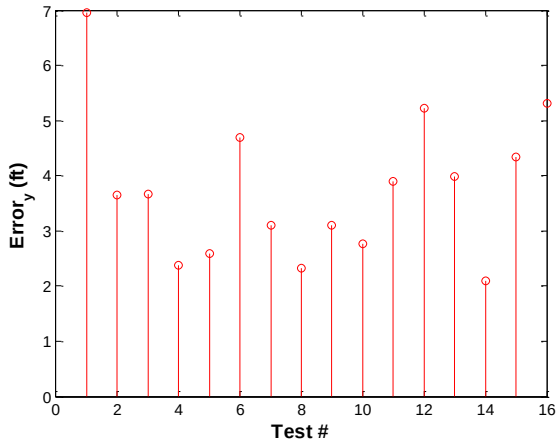

Figure 37. Localization Accuracy along Y-Axis

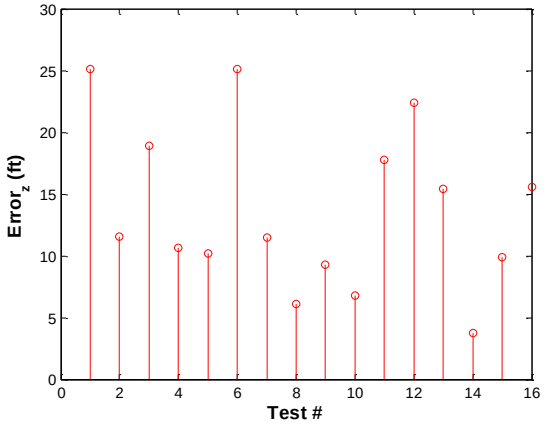

Figure 38. Localization Accuracy along Z-Axis

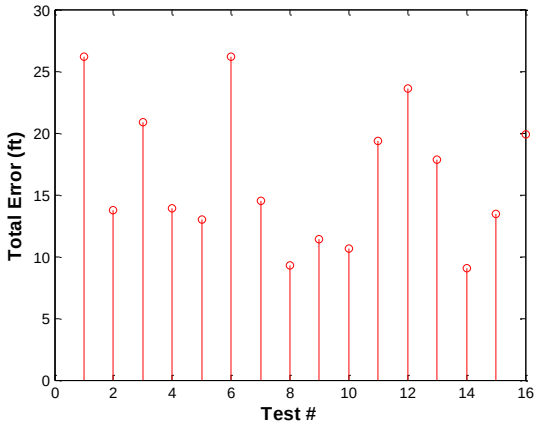

Figure 39. 3D-Position Localization Accuracy

Summary

Overall, the paper formulated a vision-based surveillance concept for airport ramp area operations. Surveillance in the ramp area can improve both safety and efficiency of the ramp area operations. The paper identified the key algorithmic modules that would be necessary for implementing the concept. Two algorithms with complimentary features were proposed for aircraft detection. An innovative approach for matching aircraft from different cameras has been identified. Sample versions of the algorithms were implemented and demonstrated on a realistic 1:400 scale model of the ramp area and aircraft. Preliminary results indicate the localization accuracy to be around 30ft which is much less than the size of the aircraft.

Challenges

The performance of the vision-based system under night-time and low-visibility conditions poses a primary challenge. The current paper does not address this issue. An infrared camera is required for handling these low-lighting scenarios. Some other challenges include high-frequency variations in illumination, camera jitter, shadows, occlusions, and the effects of ground-traffic. Another challenge is the fusion of the information resulting from the computer vision algorithms with other surveillance data.

Future Work

A significant portion of our future work involves extensive evaluation of the performance of the aircraft detection and aircraft localization algorithms using actual ramp area surveillance video data. Individual algorithmic modules are expected to be refined as part of this testing process. Work is also required for evaluating the algorithms using data from infrared cameras which are suitable for night-time and low-visibility conditions. Future work also involves formulating the data-fusion framework.

References

[1] Guilloton, A., Arenthens, J-P., Escher, A-C., Macabiau, C., and Koenig, D., “Multipath Study on

the Airport Surface," *IEEE 2012 Position Location and Navigation Symposium (PLANS)*, 23-26 April 2012, Myrtle Beach, SC, DOI: 10.1109/PLANS.2012.6236902.

[2] http://www.videosurveillance.com/traffic.asp, viewed on 8/7/2013

[3] http://www.searidgetech.com/ansp/lcgs, viewed on 8/7/2013

[4] http://www.gvdigital.com/gvdweb/html/, viewed on 8/7/2013

[5] Vaddi, S., Sweriduk, G., Kwan, J., Lin, V., Nguyen, J., and Cheng, V. H. L., "Concept and Requirements for Airport Surface Conflict Detection and Resolution," *Proceedings of the Aviation Technology Integration and Operations Conference*, Virginia Beach, Virginia, September 2011

[6] Vaddi S. S., Kwan, J., Fong, A., and Cheng, V. H. L., "Deterministic and Probabilistic Conflict Detection Algorithms for NextGen Airport Surface Operations," *Proceedings of the Guidance, Navigation, and Control Conference*, Minneapolis, Minnesota, August 2012

[7] http://flightsafety.org/asw/aug08/asw_aug08.pdf, page 44, as viewed on Sep 5, 2011.

[8] http://www.iasa.com.au/folders/Safety_Issues/RiskManagement/rampwoes.html, as viewed on Sep 5, 2011.

[9] Jung, Y. C., Hoang, T., Montoya, J., Gupta, G., Malik, W., and Toibas, L., "A Concept and Implementation of Optimized Operations of Airport Surface Traffic," *Proceedings of the 2010 AIAA Aviation, Technology, Integration and Operations Conference*, September, 2010.

[10] Evangelio, R. H., and Sikora, T, "Static Object Detection Based on a Dual Background Model and a Finite-State Machine," *Journal of Image and Video Processing*, doi:10.1155/2011/858502.

[11] Benezeth, Y., Jodoin P.-M., Emile, B., Laurent, H., and Rosenberger, C, "Comparative Study of Background Subtraction Algorithms," *Journal of Electronic Imaging*, doi:10.1117/1.3456695.

[12] P. Felzenszwalb, D. McAllester, D. Ramaman, "A Discriminatively Trained, Multiscale, Deformable Part Model," *Proceedings of the 2008 Conference on Computer Vision and Pattern Recognition*.

[13] P. Felzenszwalb, R. Girshick, D. McAllester, D. Ramanan, "Object Detection with Discriminatively Trained Part Based Models," *IEEE Transactions on Pattern Analysis and Machine Intelligence*, Vol. 32, No. 9, September 2010.

[14] Dalal, N., and Triggs, B., "Histograms of Oriented Gradients for Human Detection," *Proceedings of the 2005 Conference on Computer Vision and Pattern Recognition,* 2005.

Acknowledgements

We would like to thank Dr. Yoon Jung, Mr. Ty Hoang, Dr. Waqar Malik, Dr. Gautam Gupta, and Dr. Robert Windhorst all from NASA Ames Research Center for their inputs towards shaping the focus and content of this research.

Email Addresses

vaddi@optisyn.com

vicky@optisyn.com

miwa.hayashi@nasa.gov

Conference Identification

32nd Digital Avionics Systems Conference

October 6-10, 2013